Polyhedral control of the rhombohedral to cubic phase transition in $LaAlO_3$ perovskite



2004 J. Phys.: Condens. Matter 16 8763

(http://iopscience.iop.org/0953-8984/16/47/026)

INSTITUTE OF PHYSICS PUBLISHING JOURNAL OF PHYSICS: CONDENSED MATTER

J. Phys.: Condens. Matter **16** (2004) 8763–8773 PII: S0953-8984(04)84785-4

# Polyhedral control of the rhombohedral to cubic phase transition in $LaAlO_3$ perovskite

**J Zhao**[1], **N L Ross and R J Angel**

Crystallography Laboratory, Department of Geosciences, Virginia Polytechnic Institute and State University, Blacksburg, VA 24061, USA

E-mail: jzhao@vt.edu

Received 4 August 2004, in final form 25 October 2004
Published 12 November 2004
Online at stacks.iop.org/JPhysCM/16/8763
doi:10.1088/0953-8984/16/47/026

**Abstract**

The pressure-induced structural changes of $LaAlO_3$ perovskite, a rhombohedral perovskite with $R\bar{3}c$ symmetry, have been investigated up to 8.6 GPa in a diamond-anvil cell at room temperature using single-crystal x-ray diffraction. A fit of a third-order Birch–Murnaghan equation of state to the $P$–$V$ data yields values of $K_{T0} = 177(4)$ GPa and $K'_0 = 8.9(1.6)$. The evolution of the structure with pressure shows that compression of the $LaO_{12}$ site is strongly anisotropic, with the three longest La–O bonds being more compressible than the other nine shorter La–O bond lengths. Consequently the distortion of the $LaO_{12}$ site decreases with increasing pressure. The rotation angle around the threefold axis of the $AlO_6$ octahedra is totally determined by the relative compressibilities of the La and Al sites, and decreases significantly with pressure. This variation leads to the rhombohedral to cubic phase transition. A new model, introduced to predict the high-pressure behaviour of the $GdFeO_3$ ($Pbnm$)-type perovskites, is extended to rhombohedral perovskites in this paper. The model correctly predicts that the $AlO_6$ site is more compressible than the $LaO_{12}$ site in $LaAlO_3$, and that the rhombohedral to cubic phase transition is controlled by the relative compressibilities of the two cation sites.

## 1. Introduction

Lanthanum aluminate, $LaAlO_3$, belongs to the rhombohedral perovskite family ($R\bar{3}c$) with general stoichiometry $ABO_3$ [1–5], a framework structure with corner-linked octahedra. It deviates from the ideal cubic structure ($Pm3m$) via distortions of octahedral $BO_6$ and dodecahedral $AO_{12}$ from more regular geometry in the cubic structure [6, 7].

[1] Author to whom any correspondence should be addressed.

  

$LaAlO_3$ is of great interest in materials science, and it has become a widely used substrate material and buffer layer for high temperature superconductor (HTSC) films [8]. Its use as a substitute for silicon dioxide as a gate dielectric has also been explored [9–11]. Due to these potential applications in functional films [8–11] and its possible use as an analogue material for silicate perovskites in geosciences [12], the thermal stability of $LaAlO_3$ has been investigated. It exhibits a rhombohedral to cubic phase transition at 810 K [13–15]. The main character of the phase transition is that the angle of rotation of the $AlO_6$ octahedra continually decreases with increasing temperature until it becomes zero. The transition is second order in character.

A previous high-pressure study of $LaAlO_3$ that employed powder synchrotron x-ray diffraction and Raman spectroscopy indicated that it undergoes a rhombohedral to cubic phase transition at about 14 GPa [16]. However, the small distortion of the rhombohedral structure from cubic symmetry meant that the resolution of the powder diffraction measurements was insufficient to determine the details of the structural changes such as the tilting angle of the $AlO_6$ octahedra and the compressibilities of the bond lengths in the rhombohedral phase. High-pressure single-crystal x-ray diffraction has proved to be more effective for characterizing atomic-level compression mechanisms and structural changes in condensed systems under high pressure. However, even for single-crystal x-ray diffraction, uncertainties in high-pressure structural parameters obtained from single-crystal x-ray diffraction measurements usually make it difficult to pursue the subtle variation of polyhedra under high pressure. Recently, several improvements have been made in an attempt to reduce these uncertainties to the level approaching that obtained from crystals in air, thus enabling insights to be derived into the evolution of the distortion and tilting of polyhedra in relatively stiff materials such as the orthorhombic (*Pbnm*) oxide perovskites (see e.g. [17–20]). In this contribution, we report the results of a single-crystal x-ray diffraction study of pressure-induced structural changes of $LaAlO_3$ with emphasis on how the tilting and distortion of the $AlO_6$ octahedron changes with pressure and what atomistic factors control the relative compressibilities of the $LaO_{12}$ and $AlO_6$ sites.

## 2. Experimental methods

A synthetic $LaAlO_3$ sample was kindly supplied by the Department of Mineralogy, National Museum of Natural History. Several relatively large pieces of crystal were selected and polished to plates about 200 $\mu$m thick. After careful examination by optical microscopy and verification of the absence of twin domains, a selected plate was then polished to 30 $\mu$m, suitable for high-pressure study. X-ray diffraction measurements with a CCD detector on this plate at ambient conditions revealed no significant diffraction intensity that could be attributed to the presence of twinning. The results of a structure refinement at ambient pressure were consistent with the published data [1–5]. Then two smaller pieces (sample size: A: 116 $\mu$m $\times$ 176 $\mu$m $\times$ 30 $\mu$m; B: 154 $\mu$m $\times$ 250 $\mu$m $\times$ 30 $\mu$m) cut from the selected plate were used in two high-pressure measurements. The unit cell parameters (11 pressure points) of crystal A were used to calculate the equation of state (EoS). Although the intensity data of crystal A were collected, we only report the refinement results of crystal B (6 pressure points) because both crystals show the same refinement results within the uncertainty of measurements.

The crystal was loaded onto a 600 $\mu$m diameter culet of one anvil of an ETH diamond-anvil cell (DAC) [21]. A 4:1 methanol:ethanol mixture served as the pressure-transmitting medium. A 200 $\mu$m thick T301 steel gasket was preindented to a thickness of 90 $\mu$m and a hole (diameter $=$ 378 $\mu$m for sample A, diameter $=$ 426 $\mu$m for sample B) was drilled in the centre of the indented region. A ruby sphere was loaded into the cavity to serve as

**Table 1.** Unit cell parameters of $LaAlO_3$ perovskite at high pressure.

| $P$ (GPa) | $a$ (Å) | $c$ (Å) | $V$ (Å) |
|---|---|---|---|
| The first crystal | | | |
| 0.0001 | 5.366 01(18) | 13.109 0(6) | 326.892(25) |
| 0.59(5) | 5.359 68(10) | 13.094 9(3) | 325.771(14) |
| 1.18(7) | 5.354 09(11) | 13.082 21(22) | 324.776(15) |
| 1.74(8) | 5.348 23(13) | 13.069 3(4) | 323.745(18) |
| 2.49(5) | 5.342 00(18) | 13.054 9(6) | 322.635(25) |
| 3.21(8) | 5.335 39(17) | 13.039 4(5) | 321.458(23) |
| 3.84(6) | 5.329 65(12) | 13.027 2(4) | 320.463(17) |
| 4.66(4) | 5.322 81(13) | 13.012 5(4) | 319.281(18) |
| 5.41(1) | 5.316 08(13) | 12.997 1(5) | 318.097(18) |
| 6.07(5) | 5.311 08(12) | 12.985 6(4) | 317.219(17) |
| The second crystal | | | |
| 0.0001 | 5.366 03(15) | 13.110 5(6) | 326.86(4) |
| 1.18(5) | 5.354 33(11) | 13.083 1(4) | 324.826(16) |
| 2.78(2) | 5.339 29(11) | 13.048 0(4) | 322.137(16) |
| 4.63(8) | 5.323 31(12) | 13.010 7(5) | 319.252(24) |
| 6.81(6) | 5.305 24(24) | 12.972 20(12) | 316.21(4) |
| 8.62(5)[a] | 5.287 0(4) | 12.936 4(5) | 313.16(3) |

[a] The unit cell parameters were calculated from the EoS of $LaAlO_3$.

a pressure calibrant [22]. The uncertainty in pressure was taken as the difference between pressure measurements before and after the data collections.

The unit cell parameters were determined on a Huber four-circle diffractometer. The full details of the instrument and the peak-centring algorithms are provided in [23]. The unit cell parameters at each pressure point were determined by a least-squares fit to the corrected setting angles of 18–20 reflections obtained by the eight-position centring technique on the diffractometer [24].

Intensity data for all accessible reflections ($-7 \leqslant h \leqslant 9$, $-9 \leqslant k \leqslant 9$, $-10 \leqslant l \leqslant 10$) were collected at room pressure (in the DAC) and at 1.18, 2.78, 4.63, 6.81 and 8.62 GPa using $\omega$ scans in the fixed-$\phi$ mode [25] from 2° to 40° in $\theta$ on an Xcalibur-I diffractometer (Oxford Diffraction) equipped with Mo K$\alpha$ radiation at 50 kV and 40 mA and a point detector. We determined the offset of the crystal from the rotation axis of the goniometer by measuring 20–40 strong low-angle reflections and calculating the crystal offsets from the reflection positions with the WinIntegrStp program, v3.4 [26]. We found that it was critical to eliminate these offsets by adjusting the DAC on the goniometer before data collection. Peak fitting and integration of data collection scans were carried out by using the WinIntegrStp 3.4 software. Other data corrections including absorption by both the sample itself and the beryllium plates and diamond anvils of the DAC as well as shadowing by the gasket were made by ABSORB 6.0 [27]. After the crystallographically-equivalent reflections were averaged, the remaining independent reflections with ($F^2 > 2\sigma(F^2)$) were used to refine the structures with RFINE99, a development version of RFINE4 [28]. When the pressure was increased up to 8.62 GPa, the sample was cracked into two pieces, fewer reflections were integrated by using the WinIntegrStp 3.4 software and therefore all atoms are made isotropic for refinement. Unit cell parameters measured on the Huber diffractometer were used in the structure refinements. Details of all unit cell parameters, refinement results, the refined positions of atoms and displacement parameters and distances and angles are listed in tables 1–4.

**Table 2.** Refinement information for $LaAlO_3$ perovskite at high pressures.

| $P$ (GPa) | 0.0001 | 1.18(5) | 2.78(2) | 4.63(8) | 6.81(6) | 8.62(5) |
|---|---|---|---|---|---|---|
| $N$ ($>2I_0/\sigma(I_0)$)[a] | 383 | 371 | 375 | 366 | 357 | 236 |
| $N$ ($F^2 > 2\sigma(F^2)$)[b] | 96 | 93 | 95 | 90 | 88 | 57 |
| $R_{int}$[c] | 0.029 | 0.042 | 0.046 | 0.033 | 0.038 | 0.156 |
| $G_{fit}$[d] | 1.09 | 1.01 | 1.11 | 1.14 | 1.16 | 1.00 |
| Extinction factor ($\times 10^{-4}$) | 0.165(24) | 0.165(26) | 0.181(27) | 0.186(16) | 0.107(13) | 0.11(6) |
| $R_w$[e] | 0.027 | 0.032 | 0.027 | 0.020 | 0.024 | 0.068 |
| $R_f$[f] | 0.017 | 0.019 | 0.019 | 0.018 | 0.015 | 0.058 |

[a] Number of reflections with $I > 2I_0/\sigma(I_0)$.
[b] Number of independent reflections with $F^2 > 2\sigma(F^2)$.
[c] $R_{int}$, internal residual for symmetry-equivalent intensities.
[d] Estimated standard deviation of unit weight observation.
[e] Weighted $R_w = [\Sigma w(|F_0| - |F_c|)^2 / \Sigma |F_0|^2]^{1/2}$, weight $= (\sigma_i^2(F_i) + p^2 F_i^2)^{-2}$.
[f] Unweighted $R_f = \Sigma||F_0| - |F_c||/\Sigma|F_0|$.

**Table 3.** Unit cell parameters, refined positional parameters and anisotropic temperature factors ($U_{ij}$) and equivalent isotopic temperatures factors ($B_{eq}$) of $LaAlO_3$ perovskite at high pressure.

| $P$ (GPa) | 0.0001 | 1.18(5) | 2.78(2) | 4.63(8) | 6.81(6) | 8.62(5)[d] |
|---|---|---|---|---|---|---|
| La[a] | | | | | | |
| $B_{eq}$ | 0.60(3) | 0.68(4) | 0.61(4) | 0.60(3) | 0.56(4) | 0.64(4) |
| $U_{11}$ | 0.0066(3) | 0.0060(3) | 0.0065(3) | 0.0061(2) | 0.0061(3) | |
| $U_{33}$ | 0.0095(11) | 0.0138(15) | 0.0102(12) | 0.0105(11) | 0.0090(13) | |
| Al[b] | | | | | | |
| $B_{eq}$ | 0.66(14) | 0.70(3) | 0.48(15) | 0.56(12) | 0.56(16) | 0.56(1) |
| $U_{11}$ | 0.0050(8) | 0.0058(9) | 0.0063(10) | 0.0053(6) | 0.0060(9) | |
| $U_{33}$ | 0.015(6) | 0.013(6) | 0.006(6) | 0.011(5) | 0.009(6) | |
| O[c] | | | | | | |
| $x$ | 0.5265(5) | 0.5252(5) | 0.5243(5) | 0.5228(4) | 0.5199(4) | 0.5180(12) |
| $B_{eq}$ | 0.91(10) | 0.88(11) | 0.75(10) | 0.80(10) | 0.68(14) | 0.66(20) |
| $U_{11}$ | 0.0081(5) | 0.0077(5) | 0.0088(6) | 0.0089(6) | 0.0093(9) | |
| $U_{22}$ | 0.0141(2) | 0.0157(2) | 0.0112(2) | 0.0092(2) | 0.0094(2) | |
| $U_{33}$ | 0.013(3) | 0.013(3) | 0.009(4) | 0.012(4) | 0.006(6) | |
| $U_{23}$ | −0.0022(19) | −0.0004(12) | −0.0055(15) | −0.0021(12) | −0.0012(18) | |

[a] La: $x = 0.0$, $y = 0.0$, $z = 0.25$; $U_{22} = U_{11}$, $U_{12} = 0.5U_{11}$, $U_{13} = U_{23} = 0$.
[b] Al: $x = 0.0$, $y = 0.0$, $z = 0.0$; $U_{22} = U_{11}$, $U_{12} = 0.5U_{11}$, $U_{13} = U_{23} = 0$.
[c] O: $y = 0.0$, $z = 0.25$; $U_{12} = 0.5U_{22}$, $U_{13} = 0.5U_{23}$.
[d] All atoms are made isotropic for refinement.

## 3. Results

Figure 1(a) shows the volume of $LaAlO_3$ perovskite as a function of pressure, as measured from both crystals. Figure 1(b) displays the compression data plotted as normalized pressure, $F$, against the Eulerian strain measure, $f$ [29]. $F$–$f$ plots provide a visual indication of whether higher-order terms such as $K_0'$ and $K_0''$ are significant in the EoS. In this case the positive linear trend of the data in the $F$–$f$ plot indicates that $K_0' > 4$, and that the data should be fitted with a third-order equation of state. The fit of the $P$–$V$ data collected between room pressure and 6.07 GPa yielded room pressure parameters $V_0 = 326.889(24)$ Å$^3$, $K_{T0} = 177(4)$ GPa and $K_0' = 8.9(1.6)$ for the third-order Birch–Murnaghan equation of state with a weighted $\chi^2 = 0.51$ by using EoSFit 5.2 [29] software. The maximum difference

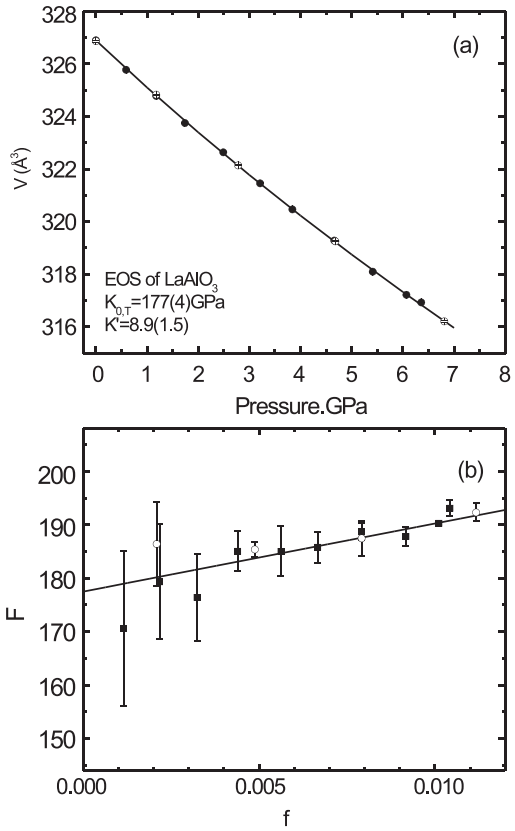


**Figure 1.** (a) Variation of the volume of $LaAlO_3$ perovskite with pressure at room pressure and (b) normalized stress–strain ($F-f$) plots derived from the measured volumes for a Birch–Murnaghan EoS (solid and open symbols present $P-V$ data of crystal A and crystal B, respectively).

**Table 4.** Interatomic distances (Å) and tilting angles $\omega$ (deg) of $LaAlO_3$ perovskite at high pressure.

| $P$ (GPa) | | 0.0001 | 1.18(5) | 2.78(2) | 4.63(8) | 6.81(6) | 8.62(5) |
|---|---|---|---|---|---|---|---|
| Al–O | $x6$ | 1.900 88(21) | 1.896 29(19) | 1.890 72(18) | 1.884 56(12) | 1.877 54(11) | 1.8702(4) |
| La–O1 i | $x3$ | 2.541(3) | 2.542(3) | 2.540(3) | 2.541(2) | 2.547(2) | 2.548(7) |
| La–O2 ii | $x6$ | 2.682 22(20) | 2.676 17(14) | 2.668 65(13) | 2.660 49(8) | 2.651 59(8) | 2.6434(3) |
| La–O2 iii | $x3$ | 2.825(3) | 2.812(3) | 2.799(3) | 2.7823(19) | 2.7580(19) | 2.738(7) |
| ∠ O–Al–O | | 90.26(1) | 90.24(1) | 90.22(1) | 90.20(0) | 90.16(0) | 90.13(1) |
| $\omega$ (deg) | | 5.24(9) | 4.99(9) | 4.81(7) | 4.49(7) | 3.95(7) | 3.57(21) |
| $\eta$ | | 0.9933 | 0.9938 | 0.9941 | 0.9947 | 0.9959 | 0.9970 |

between the experimental pressures and those calculated from the EoS is 0.072 GPa, which is within the estimated uncertainty of our ruby pressure calibration. The value of the bulk modulus is smaller than $K_{T0} = 190(5)$ GPa ($K'_0 = 7.2(4)$ and pseudo-cubic $V_0 = 54.57(3)$ Å$^3$) obtained from the previous powder synchrotron x-ray diffraction study [16]. These differences might be attributed to the fitting of the powder data with a cubic unit-cell instead of a rhombohedral one because the splitting of the pseudo-cubic diffraction maxima was not resolved in the powder diffraction patterns. The powder data also show considerably more scatter than the single-

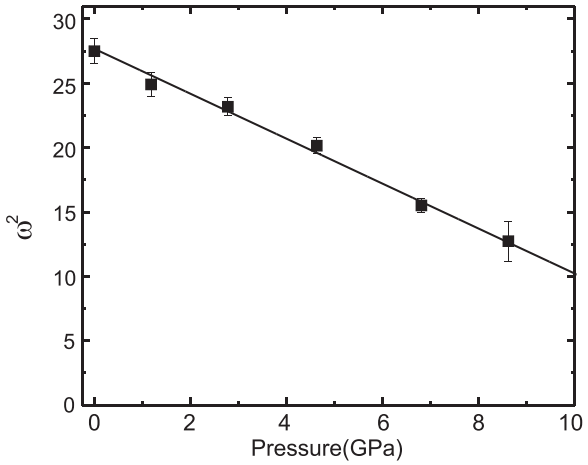


**Figure 2.** The variation of the square of the experimentally determined tilt angle $\omega$ of the $AlO_6$ octahedra as a function of pressure. The solid line is a linear fit to the data.

crystal data, with the largest misfit to the reported EoS being 0.60 GPa, which is 60 times larger than the esd in the reported data points [16].

The elastic moduli of the individual unit-cell axes of $LaAlO_3$ perovskite were obtained from the measured data by fitting a third-order Birch–Murnaghan EoS to the cubes of each of the cell parameters in turn [29]. The resulting axial moduli ($K_{d0}$) and their pressure derivatives ($K'_{d0}$) are $K_{a0} = 173(4)$ GPa and $K_{c0} = 188(5)$ GPa, with $K'_{a0} = 8.5(1.6)$ and $K'_{c0} = 9.2(2.0)$. The $c$-axis is significantly less compressible than $a$ ($=b$), and the difference in compressibility leads to a convergence of the pseudo-cubic unit-cell parameters $a/\sqrt{2}$ and $c/\sqrt{12}$ with increasing pressure and ultimately to the phase transition at 14 GPa [16].

The structural changes in $LaAlO_3$ perovskite with pressure are dominated by the overall evolution of the structure towards cubic symmetry, with the phase transition occurring at 14 GPa [16]. Thus we find that the only variable structural parameter within the structure, the fractional $x$-coordinate of the oxygen atom, decreases significantly with increasing pressure (see table 3) towards the value of $x = \frac{1}{2}$ that it would have in the cubic structure with this cell setting. The rotation angle, $\omega$, of the $AlO_6$ octahedra around the threefold axis is directly related to this coordinate by $\omega = 2\sqrt{3}(x_0 - 1/2)$ [1]. The decrease in the $x$-coordinate therefore reflects a decrease in this rotation angle towards the untilted configuration that would be found in the cubic structure. The tilt angle is the primary order parameter of the cubic to rhombohedral transition [16], and the fact that the measured variation in $\omega^2$ is approximately linear with pressure (see figure 2) supports the previous interpretation of this phase transition as being second order in character with respect to pressure [16].

The $\bar{3}$ site symmetry of the Al atom means that all of the Al–O bond lengths are equal, but the O–Al–O angles internal to the $AlO_6$ octahedra are not constrained to be 90°. With increasing pressure these angles also evolve towards the 90° (see figure 3(a)) that would be found in the cubic structure above the phase transition at 14 GPa. The octahedral distortion in rhombohedral perovskites can also be described in terms of the strain parameter $\eta = c\cos\omega/(a\sqrt{6})$ [5]. A value $\eta > 1$ indicates that the octahedra are elongated along the threefold rotation axis, $\eta < 1$ that they are compressed, and $\eta = 1$ if the octahedra are perfectly regular. The strain parameter $\eta$ for $LaAlO_3$ increases with increasing pressure (see table 4), towards unity, consistent with the evolution of the structure towards the phase transition. The compression of the $LaO_{12}$ dodecahedral site is more anisotropic, as shown in figure 3(b), as a result of the rotation of the

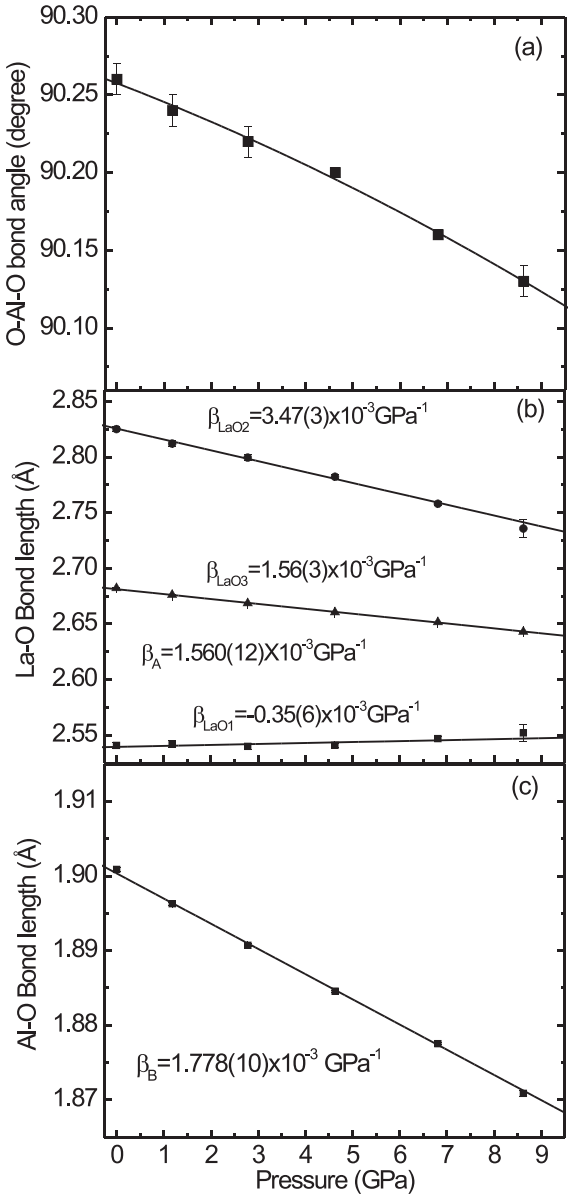


**Figure 3.** (a) The variation of the bond angle ∠ O–Al–O as a function of pressure. (b) The variation of the 12 La–O bond distances as a function of pressure. (c) The variation of the Al–O bond distance as a function of pressure.

$AlO_6$ octahedra. The three longest La–O distances are the most compressible, whereas the three shortest La–O distances show slightly negative compressibility. As a result, the distortion of the $LaO_{12}$ site decreases with increasing pressure and the bond lengths are evolving so as to become equal at the phase transition to the cubic phase. The mean linear compressibility of La–O bond ($\beta_{La-O} = 1.560(12) \times 10^{-3}$ $GPa^{-1}$) is less than that of the $AlO_6$ octahedra ($\beta_{Al-O} = 1.778(10) \times 10^{-3}$ $GPa^{-1}$: see figure 3(c)), indicating that the $LaO_{12}$ dodecahedra are less compressible than the $AlO_6$ octahedra.

## 4. Discussion

The structure of a rhombohedral perovskite is completely determined by three parameters, the $a$ and $c$ lattice parameters and the $x$-coordinate of the anion. This allows the tilt angle of the octahedra to be directly related to the volumes of the A and B sites [30]:

$$V_A/V_B = 6\cos^2\omega - 1 \tag{1}$$

where $V_A$ and $V_B$ are volumes of A site and B site polyhedra respectively. From this relationship one can deduce the following:

$$\beta_{V_B} - \beta_{V_A} = \frac{-6\sin 2\omega}{(6\cos^2\omega - 1)}\frac{\mathrm{d}\omega}{\mathrm{d}P} \tag{2}$$

where $\beta_{V_B}$ and $\beta_{V_A}$ are the volume compressibilities of the A and B site polyhedra. If we make the approximation that the volume compressibility of a site is three times the average linear compressibility of the cation–anion bonds then this becomes

$$\beta_B - \beta_A = \frac{-2\sin 2\omega}{(6\cos^2\omega - 1)}\frac{\mathrm{d}\omega}{\mathrm{d}P} \tag{3}$$

with $\beta_B$ and $\beta_A$ the linear compressibilities of the A–O and B–O bonds. Since the tilt angle $\omega$ is usually small, and always $\omega < 30°$, the term $\frac{-2\sin 2\omega}{6\cos^2\omega - 1} < 0$. This means that the pressure-induced change in the tilt angle of rhombohedral perovskites is totally determined by the relative compressibilities of the A and B sites (equation (3)). This relationship is confirmed by our experimental data for $LaAlO_3$ which shows that $\beta_B > \beta_A$ and $\mathrm{d}\omega/\mathrm{d}P < 0$. Conversely, if a rhombohedral perovskite has $BO_6$ octahedra that are stiffer than the $AO_{12}$ site then $\beta_B < \beta_A$, and the tilt angle of the octahedra would increase with increasing pressure.

The question therefore arises as to how to estimate the compressibilities or other forces involved in determining the compression behaviour of rhombohedral perovskites. Recently we used the bond-valence concept [31–34] to develop a model that successfully predicts the relative compressibilities of the cation sites in orthorhombic $GdFeO_3$-type oxide perovskites [35]. The model is based upon the assumption that the pressure-induced changes in the bond-valence sums $\Delta V_i$ at the two cation sites within any given perovskite are equal. A plot of the bond-valence sums $V_{La}$ against $V_{Al}$, as calculated from our experimentally-determined bond lengths and the published bond-valence parameters ($R_0 = 2.172$ for $La^{3+}$, 1.651 for $Al^{3+}$ [31]), shows a linear relationship as the pressure is increased up to 8.6 GPa (see figure 4). The slope of the line fitted to these valence sums is close to unity ($=1.076 \pm 0.016$). The slope is even closer to unity ($=1.007 \pm 0.014$) if the newly published value of $R_0 = 2.148$ for $La^{3+}$ [36] is used, showing that the assumption of valence matching holds for rhombohedral perovskites. Given this match of evolution of bond valences with pressure one can show that the ratio of cation site compressibilities is given by $\beta_B/\beta_A = M_A/M_B$ [35], in which the site parameter $M_i$ is defined by

$$M_i = \frac{R_i N_i}{B}\exp\left(\frac{R_0 - R_i}{B}\right) \tag{4}$$

where $N_i$ is the coordination number, $R_i$ the average bond length at room pressure, and $R_0$ and $B = 0.37$ are bond-valence parameters. The parameter $M_i$ represents the variation of the bond-valence sum at the central cation in a polyhedral site due to the change of the average bond distance.

By using bond-valence parameters and the measured bond distances at room pressure, we calculated the ratio $M_A/M_B$ of $LaAlO_3$ as 1.34 ($R_0(La^{3+}) = 2.148$ [36], $R_0(Al^{3+}) = 1.651$ [31]). Given that $M_A/M_B > 1$, the compressibility of the $AlO_6$ site should be

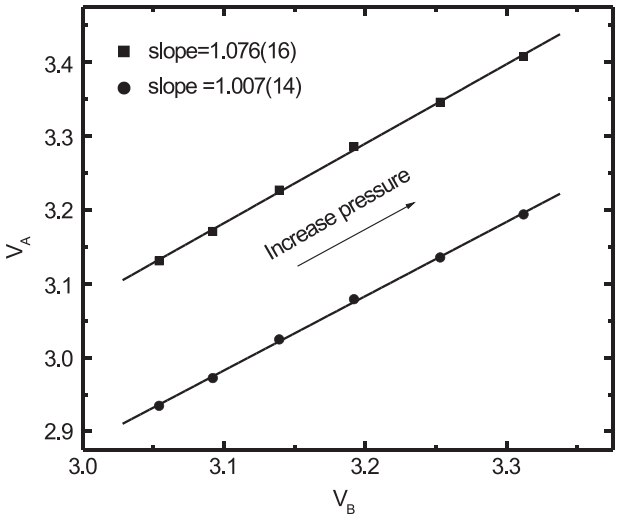


**Figure 4.** The correlation of the bond-valence sums $V_{La}$ with the bond-valence sums $V_{Al}$ in $LaAlO_3$ perovskite as a function of pressure. The upper data are calculated with bond-valence parameters $R_0 = 2.172$ for $La^{3+}$, 1.651 for $Al^{3+}$ [31], the lower data with the new bond-valence parameter for $La^{3+}$ of $R_0 = 2.148$ [36].

greater than that of the $LaO_{12}$ site, in agreement with the experimental results. Further, by analogy to the 3:3 $GdFeO_3$-type perovskites, the general prediction is that the ratio $M_A/M_B$ is greater than unity for all rhombohedral perovskites with cations of formal +3 charge [35]. Therefore the $AO_{12}$ sites are predicted to be significantly less compressible than the octahedral sites and therefore the octahedral tilts in all such perovskites should decrease with increasing pressure, leading to pressure-induced phase transitions to the cubic structure. Literature data support this conclusion. For example, the octahedral tilt of $PrAlO_3$ with $M_A/M_B = 1.25$ ($R_0(Pr^{3+}) = 2.098$ [36], $R_0(Al^{3+}) = 1.651$ [31]) decreases from 8.41° at room pressure to 5.11° at 6.25 GPa [37]. For $LaCoO_3$, $M_A/M_B = 1.50$ ($R_0(La^{3+}) = 2.148$ [36], $R_0(Co^{3+}) = 1.637$ [38]) and the experimental data show that below 4 GPa the tilting angle also decreases with pressure [39]. But above 4 GPa, the tilting angle increases with pressure due to a pressure-induced intermediate-to-low spin state transition [39] and is not consistent with the prediction of the model [35]. As we have previously noted [35], our model may not be applicable to perovskites in which the electronic structure plays a significant role in determining the distortions of the cation sites.

The magnitude of the ratio $M_A/M_B$ displays some correlation with the compressibility of the unit cell of orthorhombic perovskites. For example, the bulk moduli of Ca-perovskites $CaBO_3$ (B = Zr, Sn, Ti and Ge) show a linear correlation with $M_A/M_B$ [35] as do the 3:3 orthorhombic perovskites $AAlO_3$ (A = Sc, Y and Gd) [40]. The data available for the 3:3 rhombohedral perovskites seem to suggest a similar trend (see figure 5). The more similar the compressibilities of the $AO_{12}$ and $BO_6$ polyhedra ($M_A/M_B$ closer to unity) the higher the bulk modulus of the perovskite structure as a whole.

## 5. Conclusion

The evolution of the atomic-scale structure of $LaAlO_3$ with pressure shows that the $LaO_{12}$ site is less compressible than the $AlO_6$ site. This results in a decrease of the $AlO_6$ tilting

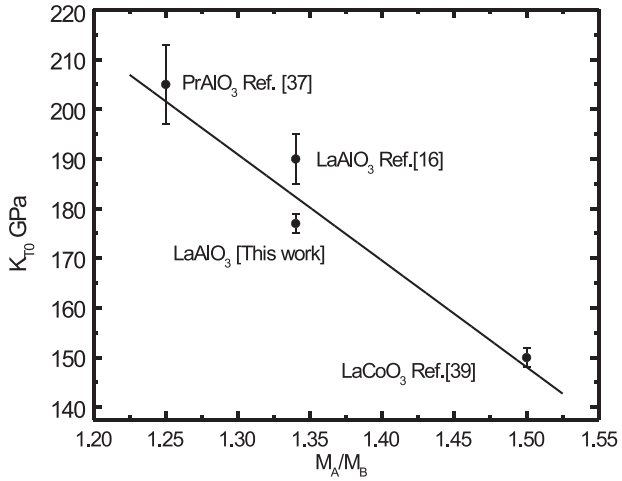


**Figure 5.** The correlation of the measured bulk moduli, $K_{T0}$, of some 3:3 rhombohedral perovskites with their $M_A/M_B$, calculated using the new bond-valence parameters for $Pr^{3+}$ and $La^{3+}$ [36].

with pressure and ultimately the pressure-induced rhombohedral-to-cubic phase transition in $LaAlO_3$ perovskite. The square of the tilt angle decreases linearly with pressure, consistent with the phase transition being second order in character. Similarly to $GdFeO_3$-type perovskites, the response of a rhombohedral perovskite to pressure can therefore be ascribed to the relative compression of the $AO_{12}$ and $BO_6$ sites. We have shown that the relative compressibilities of the two sites can be predicted by the matching relation previously derived for orthorhombic perovskites. The room pressure structure, together with bond-valence parameters, can thus be used to predict the high-pressure compressibilities and phase transitions of all rhombohedral perovskites.

## Acknowledgments

The authors acknowledge with gratitude the financial support for this work derived from NSF grant EAR-0105864. Ruby pressure measurements were conducted with the Raman system in the Vibrational Spectroscopy Laboratory in the Department of Geosciences at Virginia Tech. We thank Mr Charles Farley for his help with the Raman system.

## References

[1] Megaw H D and Darlington C N W 1975 *Acta Crystallogr.* A **31** 161
[2] de Rango C, Tsoucaris G and Zelwer C 1964 *C. R. Acad. Sci.* **259** 1537
[3] Derighetti B, Drumheller J E, Laves F, Müller K A and Waldner F 1965 *Acta Crystallogr.* **18** 557
[4] Müller K A, Berlinger W and Waldner F 1968 *Phys. Rev. Lett.* **21** 814
[5] Howard C J, Kennedy B J and Chakoumakos B C 2000 *J. Phys.: Condens. Matter* **12** 349
[6] Glazer A M 1972 *Acta Crystallogr.* B **28** 3384
[7] Woodward P M 1997 *Acta Crystallogr.* B **53** 32
[8] Lee A E, Platt C E, Burch J F, Simon R W, Goral J P and Al-Jassim M M 1990 *Appl. Phys. Lett.* **57** 2019
[9] Lu X-B, Liu Z-G, Wang Y-P, Yang Y, Wang X-P, Zhou H-W and Nguyen B-Y 2003 *J. Appl. Phys.* **94** 1229
[10] Park B-E and Ishiwara H 2003 *Appl. Phys. Lett.* **82** 1197
[11] Xiang W-F, Lu H-B, Yan L, Guo H-Z, Liu L-F, Zhou Y-L, Yang G-Z, Jiang J C, Cheng H-S and Chen Z-S 2003 *J. Appl. Phys.* **93** 533
[12] Harrison R J and Redfern S A T 2002 *Phys. Earth Planet. Inter.* **134** 253

[13] Hayward S A, Redfern S A T and Salje E K H 2002 *J. Phys.: Condens. Matter* **14** 10131
[14] O'Bryan H M, Gallagher P K, Berkstresser G W and Brandle C D 1990 *J. Mater. Res.* **5** 183
[15] Fay H and Brandle C D 1967 *J. Appl. Phys.* **38** 3405
[16] Bouvier P and Kreisel J 2002 *J. Phys.: Condens. Matter* **14** 3981
[17] Angel R J, Zhao J and Ross N L 2003 *Conf. on 'Study of Matter at Extreme Conditions' (Miami, FL, March 2003)*
[18] Ross N L, Zhao J and Angel R J 2004 *J. Solid State Chem.* **177** 1276
[19] Zhao J, Ross N L and Angel R J 2004 *Phys. Chem. Min.* **31** 299
[20] Ross N L, Zhao J and Angel R J 2004 *J. Solid State Chem.* **177** 3768
[21] Allan D R, Miletich R and Angel R J 1996 *Rev. Sci. Instrum.* **67** 840
[22] Mao H K, Xu J and Bell P M 1986 *J. Geophys. Res.* **91** 4673
[23] Angel R J, Allan D R, Miletich R and Finger L W 1997 *J. Appl. Crystallogr.* **30** 461
[24] King H E and Finger L W 1979 *J. Appl. Crystallogr.* **12** 374
[25] Finger L W and King H E 1978 *Am. Mineral.* **63** 337
[26] Angel R J 2003 *J. Appl. Crystallogr.* **36** 295
[27] Angel R J 2004 *J. Appl. Crystallogr.* **37** 486
[28] Finger L W and Prince E 1975 A system of Fortran IV computer programs for crystal structure computations *NBS Technical Note* 854 (Washington, DC: United State National Bureau of Standards) [1]
[29] Angel R J 2000 *High-Pressure, High Temperature Crystal Chemistry* (*Reviews in Mineralogy and Geochemistry* vol 41) ed R M Hazen and R T Downs (Washington, DC: Mineralogical of Society America) pp 35–59
[30] Thomas N W and Beitollahi A 1994 *Acta Crystallogr.* B **50** 549
[31] Brown I D and Altermatt D 1985 *Acta Crystallogr.* B **41** 244
[32] Brown I D 1992 *Acta Crystallogr.* B **48** 553
[33] Brown I D 1997 Bond valence methods *Computer Modeling in Inorganic Crystallography* ed C R A Catlow (New York: Academic)
[34] Brese N E and O'Keeffe M 1991 *Acta Crystallogr.* B **47** 192
[35] Zhao J, Ross N L and Angel R J 2004 *Acta Crystallogr.* B **60** 263
[36] Trzesowska A, Kruszynski R and Bartczak T J 2004 *Acta Crystallogr.* B **60** 174
[37] Kennedy B J, Vogt T, Martin C D, Parise J B and Hriljac J A 2002 *Chem. Mater.* **14** 2644
[38] Wood R M and Palenik G J 1998 *Inorg. Chem.* **37** 4194
[39] Vogt T, Hriljac J A, Hyatt N C and Woodward P 2003 *Phys. Rev.* B **67** 140401(R)
[40] Ross N L, Zhao J, Burt J A and Chaplin T D 2004 *J. Phys.: Condens. Matter* **16** 5721